Article

Sol–Gel Spin Coating Growth of Magnesium-Doped Indium Nitride Thin Films on Different Substrates

Sha Shiong Ng[1,a,*]**, Hui San Lee**[2,b]**, and Zhi Yin Lee**[2,c]

1 Institute of Nano Optoelectronics Research and Technology (INOR), Universiti Sains Malaysia, Malaysia
2 School of Physics, Universiti Sains Malaysia, 11800, USM, Penang, Malaysia
E-mail: [a,*]shashiong@yahoo.com (Corresponding author), [b]leehuisan530@yahoo.com, [c]lee_zhiyin2003@yahoo.com

Abstract. We report on the growth of p-type indium nitride (InN) thin films on different substrates using a relatively simple and cost-effective sol-gel spin coating method. The precursors for the indium source and p-type dopant were indium nitrate hydrate and magnesium chloride 6-hydrate powders, respectively. The structural, morphology, and optical properties of p-type InN thin films grown on different substrates were investigated. X-ray diffraction patterns revealed that the deposited Mg-doped InN thin film on GaN/AlN/Si(111) template show polycrystalline wurtzite structure with a strong InN(002) orientation and have a good crystallinity. Field emission scanning electron microscopy images and energy dispersive X-ray results showed that all the films exhibit densely packed surface morphology with hexagonal-like grains shape and low oxygen percentage with almost 1:1 ratio of indium to nitrogen. Moreover, two Raman-active modes of E_2(High) and A_1(LO) of the wurtzite InN were clearly observed for all samples. The ultraviolet-visible-near infrared spectroscopy results showed that the energy bandgap of the Mg-doped InN thin films was in the range of 1.62-1.66 eV. From all the results, it can be concluded that the Mg doped InN film on GaN/AlN/Si(111) substrate has better crystalline quality as compared to that of other substrates.

Keywords: Indium nitride, Kubelka-Munk function, magnesium dopant, nitridation process, sol-gel spin coating.

1. Introduction

In recent years, the remarkable optical properties exhibited by InN have attracted great research interest. The re-evaluation of the InN bandgap to 0.7 eV allows continuous change of the InGaN alloy bandgap from 0.7 eV to 3.4 eV [1]. Subsequently, the bandgap energies of InGaN alloy system cover the entire visible and part of the near ultra-violet spectral regions. This spark an immense scientific interest to develop high-efficiency InGaN based solar cell compared to conventional silicon or cadmium telluride structure. Nevertheless. the development related to this material system is still in an early stage. There are still challenge and limitation that need to overcome. For instance, the growth of high-quality InN (as well as In-rich InGaN) films [2] and the growth of p-type doping [3] are still difficult.

It is known that the synthesis of InN is considered the most challenging among the III-nitride compounds. This is mainly due to high equilibrium nitrogen vapor pressure [4], low dissociation temperature (around 630 °C) of the InN [4], lack of lattice-matching substrates, and difficulty to prepare in stoichiometric form [4, 5]. Several studies reported that the thermal stability is one of the critical factors affecting the InN crystal growth. At high growth temperatures, the metallic-indium tends to dissociate from the crystal. Thus, to prevent the thermal decomposition of InN, researchers proposed to grow InN at low temperatures [6, 7]. However, the low growth temperature has resulted in the deficiency of active nitrogen (N) atoms and reduction of the kinetic energies of the reactants in forming InN bonds [8].

Typically, advanced deposition techniques such as metal-organic chemical vapor deposition (MOCVD), molecular beam epitaxy (MBE), plasma-assisted reactive evaporation, and reactive sputtering, etc. have been developed to grow high crystallinity InN thin films [5, 9]. However, researchers are still encountered difficulty in growing good quality InN thin films. For instance, the researchers were only able to obtain the nanocrystalline InN thin films using reactive sputtering technique at different nitrogen and argon gases ratios [10, 11]. While the MOCVD method was restricted by the low growth temperature of InN. This leads to a low decomposition rate of the ammonia gas and hence, low growth rate of the InN [4]. In addition, the crystallinity of MOCVD growth InN is strongly dependent on the V/III source ratio, where the lack of either one source will lead to the formation of indium droplets [9, 12]. On the other hand, the MBE growth is dependent upon the atomic species being deposited. To overcome the problem of atomic impurities, an ultrahigh vacuum system is required to remove the unwanted background gases, such as oxygen, which causes defects on the deposited thin films [13].

For the growth of p-type InN thin films, one of the difficulties is the solubility of doping InN with Mg. Due to the low dissociation temperature of the InN, the growth is normally performed under temperature not higher than ~630 °C. As a result, the solubility of the Mg dopant is low, and the doping is difficult [14]. There are few researchers have successfully grown p-type InN by using MBE methods. For example, Wang et al. (2011) [15] reported on Mg doped InN grown by radio-frequency plasma-assisted MBE and successfully proved the present of free holes in InN. Besides that, Jone et al. (2006) [16] have reported a systematic investigation on Mg-doped InN by MBE method. The growth of Mg-doped InN thin films using MOCVD method is rather difficult due to the high temperature growth nature of the MOCVD and the issue of unintentional dopants. Impurities such as oxygen and hydrogen (H) are sources of these unintentional dopants. It was suggested that oxygen is the source of native donors in InN, instead of nitrogen vacancies. Hydrogen is often used as a carrier gas for the sources in MOCVD systems. It reacts with Mg atoms to form Mg-H strong bond dopants in InN. This phenomenon is known as passivation of acceptor. As more Mg atoms are successfully incorporated into the lattice without exceeding the solubility limit, more H is also incorporated to passivate the Mg. Nevertheless, the Mg can later be activated thermally in a nitrogen gas environment. Under this condition, the strong Mg-H bond can be broken easily [17].

Although undoped and Mg-doped InN has been successfully grown by MBE and MOCVD, but all these techniques involve complicated setup and relatively expensive. Moreover, some growth techniques use metal organic and hydride precursors which are volatile and extremely dangerous. Therefore, an alternative growth method which is simpler, safer, and cheaper is highly needed. Recently, we have successfully grown InN [18-20] and Mg-doped InN [21-23] using sol-gel spin coating technique. This approach allows the growth below the decomposition temperature of the InN (i.e., around 630 °C). In addition, the sol-gel spin coating approach is relatively simple, i.e., it uses chemical solution (precursor) to produce (undoped and doped) thin and uniform films. Subsequently, the sol-gel spin coating method is a potential approach for producing undoped and doped InN thin films.

Up to now, there are no studies on p-type InN films deposited on various substrates. The substrate is very important for the growth of p-type InN thin films because a suitable substrate not only can improve the structural properties of film but also can enhanced the optical and electrical properties of the films [24]. However, there are few challenges in growth of Mg-doped InN on different substrates in terms of the lattice and thermal mismatching between film and the substrate because it commonly leads to the development of stress in the deposited film. Other than that, nucleation and binding of the growth species might vary due to the different substrate properties [25]. Those challenges can affect crystalline quality as well as optical and electrical properties of Mg-doped InN film.

From the literature review, sapphire is the most extensively used substrate for growth of the III–nitrides despite of its large structural and thermal mismatch with InN. The lattice mismatch between the InN and sapphire is approximately 25% [26]. While the lattice mismatch

between the InN and Si (111) substrate is about 8%. Although silicon has smaller lattice mismatch, but SiNx interfacial layers formed during the growth can cause poor crystalline quality on the deposited InN film [27]. The aforementioned substrate problems can be solved by using GaN and AlN buffer layers which can reduce the lattice mismatch and improve the structural and electrical properties of Mg-doped InN [5].

In this work, we report on the sol-gel spin coating growth of Mg-doped InN thin films on aluminium nitride on sapphire (AlN/Al$_2$O$_3$), gallium nitride on aluminium nitride on silicon [GaN/AlN/Si(111)], and aluminium nitride on silicon [AlN/Si(111)] substrates. The objective of this work is to investigate the effects of the substrate on the structural, morphology, and optical properties of the deposited Mg-doped InN thin films. From all the results, it can be found that the Mg-doped InN film on GaN/AlN/Si (111) substrate has better crystalline quality as compared to that of other substrates. Through this study, it is hope that a better understanding of the correlation between the material's properties and the type of substrates can be obtained. Eventually, the findings may lead to the realization of high efficiency InN-based solar cells. Thus, helps to meet the energy demand of future generations.

2. Experimental Details

In this works, the good quality AlN/Al$_2$O$_3$, GaN/AlN/Si(111), and AlN/Si(111) substrates obtained from Kyma Technologies Inc. were used. These substrates were first cut into the dimension of 1 cm x 1 cm and were cleaned by immersing it into the chemical solution of hydrofluoric acid and distilled water with a ratio of 1:50 for 20 s to remove a native oxide layer. Then, the substrates were rinsed with distilled water and dried with nitrogen gas following by plasma treatment to enhance wetting process. Plasma system (PlasmaPrep 100) was used for substrate surface treatment. The plasma treatment was carried out under atmospheric plasma ambient at 40 W of power and 100 °C of temperature for 10 min.

Indium nitrate hydrate [In(NO$_3$)$_3$xH$_2$O, purity 99.99%] and magnesium chloride 6-hydrate [MgCl$_2$·6H$_2$O, purity 98%] powders were dissolved in the ethanol (purity 99.7 %) followed with ultrasonic agitation. The prepared precursor was dropped onto the substrates and rotated for 25 s at 2000 rpm using spin coater. This process was repeated for several times as to achieve a desired thickness. To refine and dry the deposited films, annealing process was carried out at 300 °C for two hours. Finally, the nitridation process was carried out in order to transform the deposited film to InN. The nitridation process was conducted in furnace under ammonia and nitrogen atmosphere for 45 min with a constant flow rate of 400 sccm and 60 sccm, respectively, as shown in Fig. 1. During the nitridation process, both gases were flowed simultaneously into the furnace. After the nitridation, the sample was cooled down in room temperature.
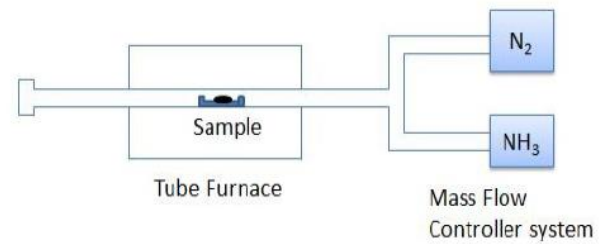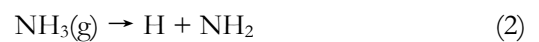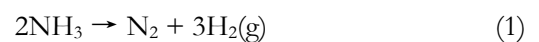

Fig. 1. Schematic diagram of custom-made furnace system used for the nitridation process.

In this work, the furnace was set at 600 °C to break ammonia bond and generate active nitrogen radicals for chemical reaction purpose. The chemical reaction equations for formation of InN can be summarized as:

$$2NH_3 \rightarrow N_2 + 3H_2(g) \tag{1}$$

$$NH_3(g) \rightarrow H + NH_2 \tag{2}$$

$$In_2O_3(s) + 2NH_3(g) \rightarrow 2InN(g, s) + 3H_2O(g) \tag{3}$$

The crystalline structure, surface morphologies, and element compositions of the Mg-doped InN thin films were investigated by using high resolution X-Ray diffractometer system (HR-XRD PANanalytical X'Pert PRO MRD PW3040), field-emission scanning electron microscopy (FESEM, FEI Nova NanoSEM 450 system), and energy dispersive X-ray (EDX) spectroscopy which attached to FESEM system, respectively. The lattice vibrational properties of the deposited thin films were accessed using Raman spectroscopy (Horiba Jobin–Yvon HR800UV). Lastly, the energy band gap of the Mg doped InN thin films was determined by using the ultraviolet-visible-near infrared spectrometer (UV-Vis-NIR, Agilent Cary 5000).

3. Results and Discussion

Figure 2 shows the XRD patterns of Mg-doped InN thin films grown on different substrates. The polycrystalline structure can be clearly observed for Mg-doped InN thin film grown on different substrates. Three dominant diffraction peaks can be observed in three different substrates, which are the characteristics of the InN(100), InN(002) and InN(101) peaks, respectively. All the diffraction peaks were ascribed to the formation of wurtzite structure InN (JCPDS file ID 03-065-3412). This result indicates that the sol-gel process yields wurtzite hexagonal InN. No other impurity from elemental metallic In and, In$_2$O$_3$ were found in the XRD patterns. Other than that, we observed the intensity of the InN(002) diffraction peak for Mg-doped InN deposited on GaN/AlN/Si(111) substrate is about 10 times highest than that of the others two substrates. This indicating that a highly c-axis oriented InN(002) was formed on

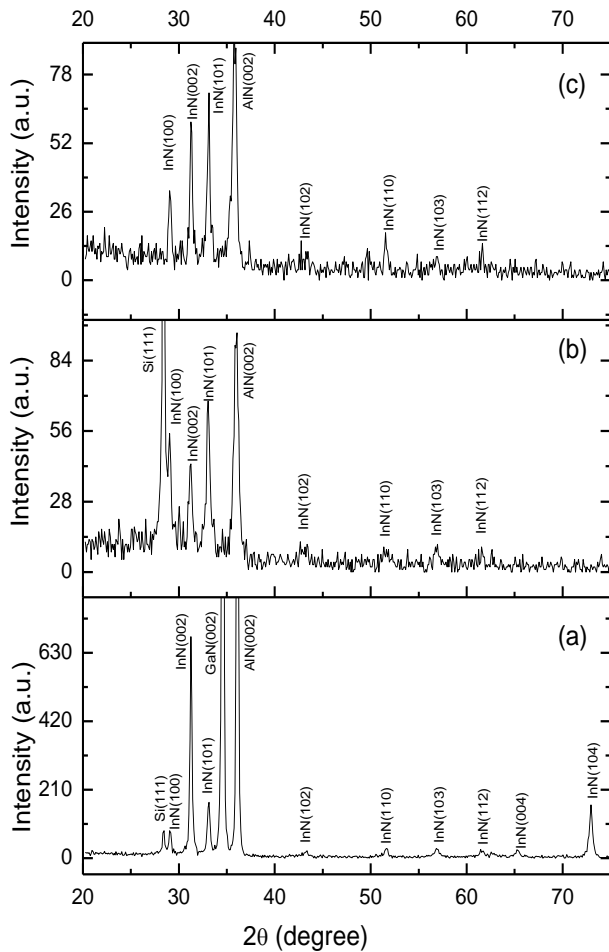GaN/AlN/Si(111) substrate. This result was in good agreement with that reported by Chen et al., (2006) [28].

Fig. 2. XRD patterns of Mg-doped InN thin films grown on (a) GaN/AlN/Si(111), (b) AlN/Si(111), and (c) AlN/Al$_2$O$_3$ substrates.

To calculate the average crystallite size (D) of the samples, Debye-Scherrer equation was used:

$$D = \frac{K\lambda}{B\cos\theta} .\qquad(4)$$

Here the K is crystallite shape factor (0.94), λ is the X-ray wavelength, B is the full width at half the maximum (FWHM) in radians, and θ is the Braggs' angle in degree [29]. The obtained results were summarized in Table 1. From Table 1, it can be found that the crystallite sizes of the Mg-doped InN films were in the range of 25.35 nm to 39.18 nm. By comparing the FWHM and the calculated crystalline size values shown in Table 1, it can be deduced that the Mg-doped InN films which grew on GaN/AlN/Si(111) has the best crystalline structure.

The lattice parameters a and c values for the films were calculated using:

$$\frac{1}{d_{hkl}^2} = \frac{4}{3}\frac{h^2+hk+k^2}{a^2} + \frac{l^2}{c^2} ,\qquad(5)$$

where d is the inter-planar distance, and h, k, l are the Miller Indices [29]. The values of calculated lattice parameter were tabulated in Table 1. The obtained a and c lattice parameters were observed to be slightly different among these three substrates, which evidenced that the lattice parameters were influenced by the type of substrates or in other words the lattice matching between the film and the substrate.

The lattice mismatch between film and substrate will lead to strain in the film. Subsequently, this results to the formation of dislocations (defects) in the films and causes degradation of the crystalline quality of deposited films. The strain (ε) in the film can be calculated using:

$$\varepsilon = \frac{(c-c_0)}{c_0} ,\qquad(6)$$

where, the c_0 is the lattice parameter for strain-free films.

The dislocation density (δ) is described as the length of dislocation lines per unit volume of the crystal [2]. The δ for preferential orientation is given by:

$$\delta = 1/D^2 ,\qquad(7)$$

where D is the crystallite size of the InN(002) [30]. All the obtained results are summarized in Table 1.

Table 1. Full-width at half maximum (FWHM), crystalline size, lattice parameters, strain, and dislocation density of Mg-doped InN grown on GaN/AlN/Si(111), AlN/Si(111), and AlN/Al$_2$O$_3$ substrates.

	GaN/ AlN/ Si(111)	AlN/ Si(111)	AlN/ Al$_2$O$_3$
FWHM (°)	0.22	0.34	0.25
Crystalline Size, D (nm)	39.18	25.35	34.48
Lattice Parameters (Å)	a= 3.543 c= 5.740	a= 3.547 c= 5.744	a= 3.545 c= 5.742
Lattice Mismatch	0.64	0.71	0.68
Dislocation Density	6.51	15.5	8.41

From Table 1, the c-lattice constant obtained for all samples is larger than that of the strain-free c-lattice constant (5.7033 Å) [31]. This means that all the deposited InN films are under the state of tensile strain. In addition, it is also found that the Mg-doped InN film deposited on GaN/AlN/Si(111) substrate shows the lowest strain and smallest dislocation density as compared to that of the other two substrates. It was suggested that the hexagonal structure of GaN buffer layer can probably help in stress relaxation at the InN/GaN interface [32]. The smaller

dislocation density indicates low concentration of lattice imperfections which leads to better formation of InN crystallization on GaN/AlN/Si (111) substrate. Based on above discussion, the Mg-doped InN film deposited on GaN/AlN/Si(111) substrate have better crystalline properties than those prepared on AlN/Si(111) and AlN/Al$_2$O$_3$ substrates.

Figure 3 shows the plan-view FESEM images of Mg-doped InN thin films deposited on different substrates captured with low magnification (×10 kx). While the inset show the corresponding plan-view FESEM images captured with high magnification (×100 kx). From Fig. 3(c), it can be seen that the Mg-doped InN thin film deposited on AlN/Si (111) substrates shows the flat and plane surface morphologies. This might be due to the large lattice mismatch of Mg-doped InN film with the substrate and lead to misfit dislocations which can impinge the growth rate of the grains. On the other hand, Mg doped InN thin films deposited on GaN/AlN/Si(111) substrates shows the largest island morphology with hexagonal symmetry. This observation indicating that strain was almost relaxed which promotes the growth rate of the grains [33]. Based on above discussion, the Mg doped InN film deposited on GaN/AlN/Si substrate shows largest hexagonal shape grain and should have better crystalline properties than those prepared on AlN/Si(111) and AlN/Al$_2$O$_3$ substrates.

The EDX measurements were carried to access and identify the elemental composition of the deposited thin films, as shown in Fig. 4. The obtained data shows that Mg-doped InN thin films deposited on GaN/AlN/Si(111) substrate has the highest atomic percentage ratio of indium to nitrogen. This observation indicating that GaN/AlN/Si(111) substrate has less lattice mismatch that almost relaxed to promote the growth of InN. Besides, the oxygen (O) atomic percentage for AlN/Al$_2$O$_3$ substrate was higher than AlN/Si(111) and GaN/AlN/Si(111). The O atoms might originate from the substrate itself.

Figure 5 shows the Raman spectra of Mg-doped InN films deposited on different substrates measured at $z(x, x)\bar{z}$ configuration, where the z-axis is parallel to the c-axis of InN. The probing laser wavelength is 514 nm. The Raman position of each active mode was determined using the Lorentzian line shape fitting. From Fig. 5, the present of A$_1$(LO) and E$_2$(High) modes at all samples indicating the deposited InN films have wurtzite structure. Due to the tensile strain, the Raman peak for InN E$_2$(high) and A$_1$(LO) modes were red shifted from 490 cm^{-1} and 586 cm^{-1} for GaN/AlN/Si(111) to 483 cm^{-1} and 578 cm^{-1} for AlN/Si(111). The full widths at half maximum (FWHM) for A$_1$(LO) mode for GaN/AlN/Si(111), AlN/Si(111), and AlN/Al$_2$O$_3$ substrates were 35 cm^{-1}, 50 cm^{-1}, and 43 cm^{-1}, respectively. Furthermore, the FWHM for E$_2$(high) mode for GaN/AlN/Si(111), AlN/Si(111), and AlN/Al$_2$O$_3$ substrates were 60 cm^{-1}, 80 cm^{-1}, and 65 cm^{-1}, respectively. The smallest FWHM value for InN film grown on GaN/AlN/Si(111) substrate indicates a good crystallite quality than that of the other two substrates.
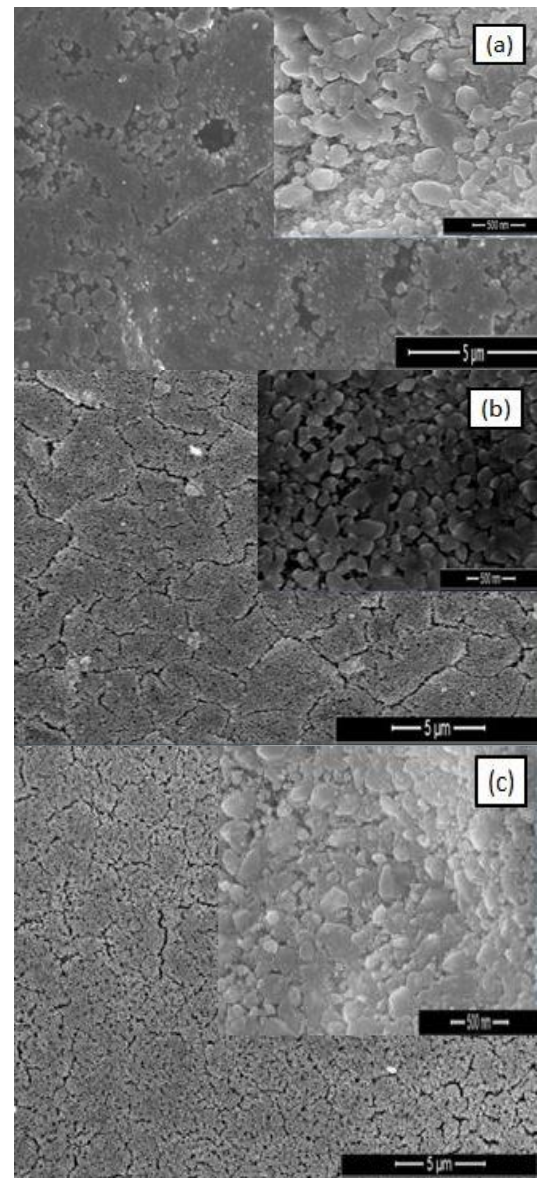

Fig. 3. FESEM images of Mg-doped InN thin films deposited on (a) GaN/AlN/Si(111), (b) AlN/Al$_2$O$_3$, and (c) AlN/Si(111) substrate. Inset is the FESEM images captured with at high magnification (×100 kx).
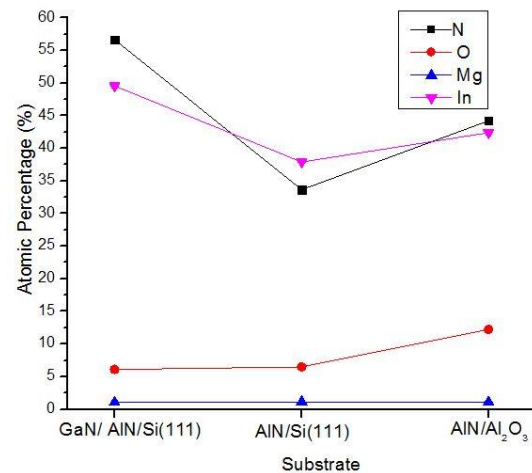

Fig. 4. EDX results of Mg-doped InN thin films deposited on different substrates.

This result is good agreement with XRD results as discussed previously [34]. In Fig. 5, a weak Raman peak around 562 cm⁻¹ which corresponding to ν4 vibration of the MgN₄ tetrahedron (labelled as ♣) can be observed in all the Rama spectra of the Mg-doped InN films. This mode assigned to local vibration mode (LVM) of magnesium that substitute InN (Mg-N) [35].
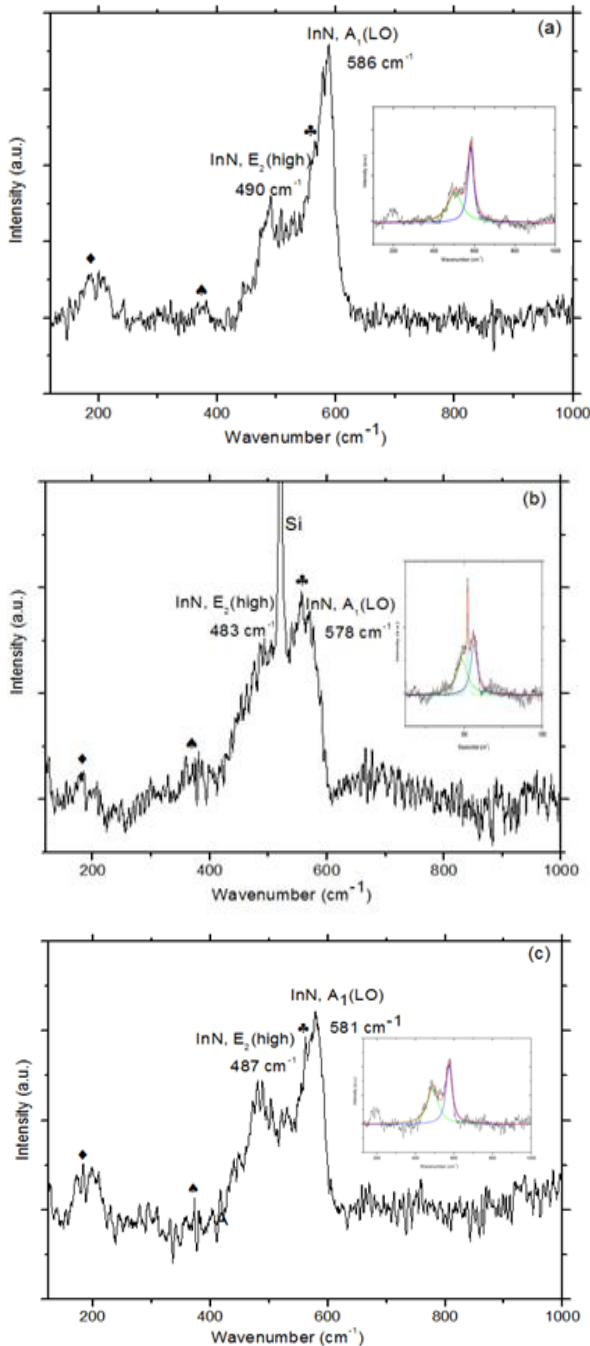

Fig. 5. Raman spectra for Mg-doped InN deposited on GaN/AlN/Si(111), AlN/Si(111), and AlN/Al₂O₃ substrates.

To further verify the Raman peak of LVM of Mg-N, the theoretical LVM frequencies of the Mg-N were calculated using:

$$\frac{\omega_{InN}}{\omega_{LvM}} = \sqrt{\frac{\mu_{LvM}}{\mu_{InN}}} \qquad (8)$$

where the reduced masses, μ_{LVM} and μ_{InN} were calculated using following equations:

$$\mu_{LVM} = \frac{m_{Mg}\,m_N}{m_{Mg} + m_N} \qquad (9)$$

$$\mu_{InN} = \frac{m_{In}\,m_N}{m_{In} + m_N}. \qquad (10)$$

Here, the m_{Mg} is the atomic mass of Mg (24.305u), m_N is the atomic mass of N (14.0067u) and m_{In} is the atomic mass of In (114.818u). We assumed that the Mg atom is incorporated on In lattice site and using theoretical value of $\omega_{InN} = \omega[E1(TO)] = 477$cm⁻¹ [21], a value of 565 cm⁻¹ for Mg-N vibration can be obtained, which is in good agreement with the experimental value of 562 cm⁻¹. Thus, using this theoretical calculation, it has been proved that our experimental value of 562 cm⁻¹ can be attributed to LVM of Mg-N [21]. The Raman peaks at 180 cm⁻¹ represented by the symbol ♠ and 369 cm⁻¹ represented by the symbol ♦ shown in Fig. 5(a, b, c) indicating the N and In vacancies, respectively. Therefore, the obtained LVM, N vacancies and In vacancies can further evidence that the existed of compensation of In-N-Mg bonding.

Figure 6 shows the Kubelka–Munk function of Mg-doped InN deposited on GaN/AlN/Si(111), AlN/Si(111), and AlN/Al₂O₃ substrates. The bandgap energy of the Mg-doped InN grown on different substrates can be estimated by the intercept of the tangent to the plot of (F(R)$h\nu$)² vs. ($h\nu$). The optical bandgap energy E_g can be estimated using:

$$F(R)h\nu = A(h\nu - E_g)^n \qquad (11)$$

where A is the proportionality constant and $h\nu$ is the photon energy, R is the reflectance value [36]. For a direct bandgap semiconductor, $n = \frac{1}{2}$ [36]. The Kubelka-Munk function F(R) coefficient can be calculated by using:

$$F(R) = \frac{(1-R)^2}{2R} \qquad (12)$$

The bandgap energy of Mg-doped InN on GaN/AlN/Si(111), AlN/Si(111), and AlN/Al₂O₃ substrates were found to be 1.62 eV, 1.66 eV, and 1.64 eV, respectively. Pan et al. [37] proved the optical bandgap value of indium oxide grown by thermal evaporation technique was approximately ≃3.56 eV. Therefore, the obtained optical bandgap values of 1.62 – 1.66 eV are further verified that the main bonding in the deposited film is In-N but not indium oxide impurities. From the Figure 6, it is clearly seen that the bandgap decreases with the sequence of AlN/Si(111) > AlN/Al₂O₃ > GaN/AlN/Si(111) substrates. The shift of the energy bandgap of Mg-doped InN deposited on AlN/Al₂O₃ and AlN/Si(111) substrates can be explained by the defects as

grain boundaries [38, 39]. As compared to the reported optical bandgap for undoped InN (i.e., 1.9 eV) [40], it was found that the obtained bandgap energies for the Mg-doped InN films are redshifted of 0.28 – 0. 24 eV. This redshifted behavior can be attributed to the present of Mg dopants. In generally, the Mg dopants will contribute excessive holes carriers and act as acceptor impurities. Consequently, an energy level was formed near the valence band edge. Hence, the effective energy bandgap of the Mg-doped InN films is lower than the undoped InN films.
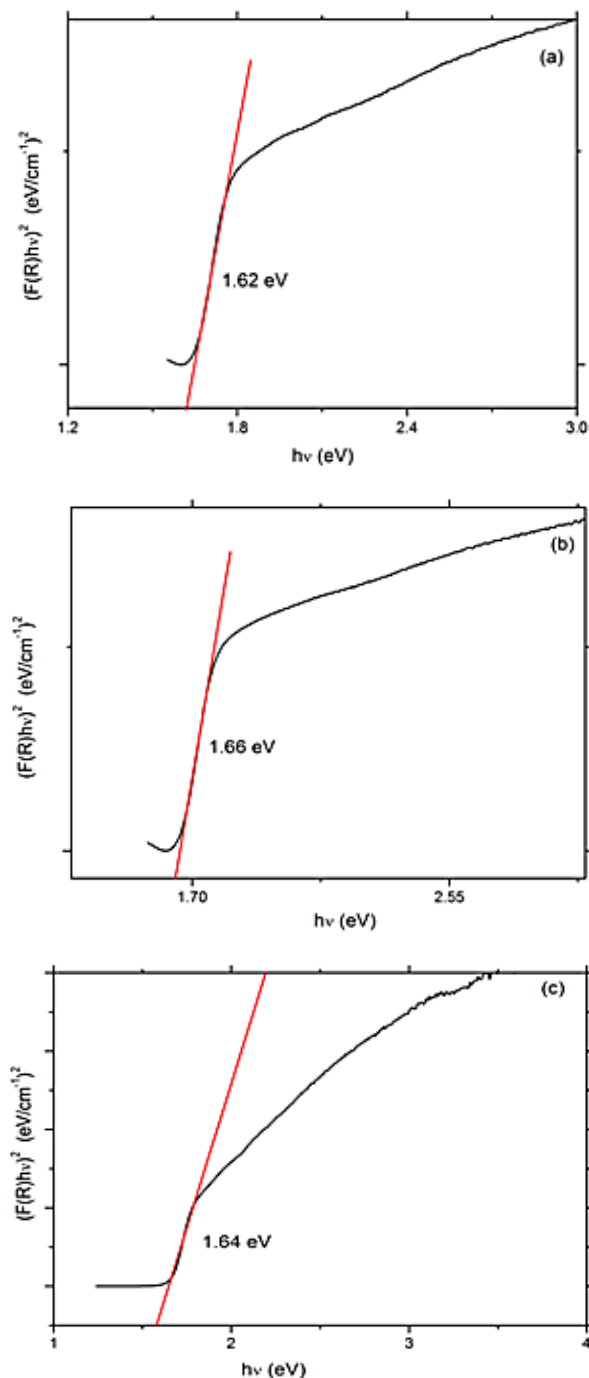

Fig. 6. Kubelka–Munk function used to calculate the energy bandgap of the Mg-doped InN deposited on (a) GaN/AlN/Si(111), (b) AlN/Si(111), and (c) AlN/Al$_2$O$_3$ substrates.

4. Conclusion

In summary, wurzite structure Mg-doped InN thin films were successfully deposited on GaN/AlN/Si(111), AlN/Si(111), and AlN/Al$_2$O$_3$ substrates using sol-gel spin coating method, a relative simple and cost-effective method. All the results revealed that the Mg-doped InN films deposited on GaN/AlN/Si(111) substrate has the best crystalline quality. Finally, it was found that the energies bandgap of the sol-gel spin coating growth of Mg-doped InN films on different substrates are in the range of 1.62 eV – 1.66 eV.

References

[1] J. Wu, W. Walukiewicz, K. M. Yu, J. W. Ager, E. E. Haller, H. Lu, W. J. Schaff, Y. Saito, and Y. Nanishi, "Unusual properties of the fundamental band gap of InN," *Appl. Phys. Lett*, vol. 80, no. 21, pp. 3967–3969, 2002.

[2] I. H. Ho and G. B. Stringfellow, "Solid phase immiscibility in GaInN," *Appl. Phys. Lett.*, vol. 69, no. 18, pp. 2701–2703, 1996.

[3] K. Kumakura, T. Makimoto, and N. Kobayashi, "Mg-acceptor activation mechanism and transport characteristics in p-type InGaN grown by metalorganic vapor phase epitaxy," *J. Appl. Phys.*, vol. 93, no. 6, pp. 3370–3375, 2003.

[4] J. B., MacChesney, P. M., Bridenbaugh, and P. B., O'Connor, "Thermal stability of indium nitride at elevated temperatures and nitrogen pressures," *Mater. Res. Bull.*, vol. 5, no. 9, pp. 783-792, 1970.

[5] W. C. Chen and S. Y. Kuo, "Study of high quality indium nitride films grown on Si(100) substrate by RF-MOMBE with GZO and AlN buffer layers," *J. Nanomater.*, vol. 2012, p. 853021, 2012.

[6] Z. Chen, Y. Li, C. Cao, S. Zhao, S. Fathololoumi, Z. Mi, and X. Xu, "Large-scale cubic InN nanocrystals by a combined solution- and vapor-phase method under silica confinement," *J. Am. Chem. Soc.*, vol. 134, no. 2, pp. 780-783, 2012.

[7] L. Gao, Q. Zhang, and J. Li, "Preparation of ultrafine InN powder by the nitridation of In$_2$O$_3$ or In(OH)$_3$ and its thermal stability," *J. Mater. Chem.*, vol. 13, no. 1, pp. 154-158, 2003.

[8] F. Stokker-Cheregi, A. Nedelcea, F. M. Voicu, D. M. Marin, R. Birjega, and M. Dinescu, "Structure and morphology of indium nitride thin films grown by plasma assisted PLD: The impact of nitrogen flow and substrate temperature," *Rom. Rep. Phys.*, vol. 65, no. 1, pp. 213-218, 2013.

[9] Ö. Tuna, H. Behmenburg, C. Giesen, H. Kalisch, R. H. Jansen, G. P. Yablonskii, and M. Heuken, "Dependence of InN properties on MOCVD growth parameters," *Phys. Status Solidi C*, vol. 8, no. 7-8, pp. 2044-2046, 2011.

[10] L. Braic and N. C. Zoita, "Influence of the deposition time and temperature on the texture of InN thin films grown by RF-magnetron sputtering," *OAM-RC*, vol. 4, no. 12, pp. 2013-2017, 2010.

[11] M. Amirhoseiny, Z. Hassan, S. S. Ng, and M. A. Ahmad, "Characterizations of InN thin films grown on Si (110) substrate by reactive sputtering," *J. Nano Mat.*, vol. 24, p. 579427, 2011.

[12] A. C. Jones, "MOCVD of electroceramic oxides: A precursor manufacturer's perspective," *Chem. Vap. Deposition*, vol. 4, no. 5, pp. 169-179, 1998.

[13] S. Mukundan, L. Mohan, G. Chandan, B. Roul, S. B. Krupanidhi, S. Shinde, K. K. Nanda, R. Maiti, and S. K. Ray, "High indium non-polar InGaN clusters with infrared sensitivity grown by PAMBE," *AIP Adv.*, vol. 5, no. 3, p. 037112, 2015.

[14] E. Cimpoiasu, E. Stern, R. Klie, R. A. Munden, G. Cheng, M. A. and M. A. Reed, "The effect of Mg doping on GaN nanowires," *Nanotechnology*, vol. 17, no. 23, p. 5735, 2006.

[15] K. Wang, N. Miller, R. Iwamoto, T. Yamaguchi, M. A. Mayer, T. Araki, Y. Nanishi, K. M. Yu, E. E. Haller, W. Walukiewicz, and J. W. Ager, "Mg doped InN and confirmation of free holes in InN," *Appl. Phys. Lett.*, vol. 98, no. 4, p. 042104, 2011.

[16] R. E. Jones, K. M. Yu, S. X. Li, W. Walukiewicz, J. W. Ager, E. E. Haller, H. Lu, and W. J. Schaff, "Evidence for p-type doping of InN," *Phys. Rev. Lett.*, vol. 96, no. 12, p. 125505, 2006.

[17] S. Nakamura, T. Mukai, M. Senoh, and N. Iwasa, "Thermal annealing effects on p-type Mg-doped GaN films," *Jpn. J. Appl. Phys.*, vol. 31, part 2, no. 2B, pp. L139–L142, 1992.

[18] Z. Y. Lee, S. S. Ng, F. K. Yam, and Z. Hassan, "Effects of coating cycles on spin-coated indium nitride thin films," *Surf. Eng.*, vol. 34, no, 7, pp. 554-561, 2018.

[19] Z. Y. Lee, S. S. Ng, and F. K. Yam, "Growth mechanism of indium nitride via sol-gel spin coating method and nitridation process," *Surf. Coat. Tech.*, vol. 310, pp. 38-42, 2017.

[20] Z. Y. Lee, S. S. Ng, and F. K. Yam, "Influences of elevated thermal decomposition of ammonia gas on indium nitride grown by sol-gel spin coating method," *Mater. Res. Bull.*, vol. 96, part 3, pp. 258-261, 2017.

[21] H. S. Lee, S. S. Ng, and F. K. Yam, "Sol–gel spin coating growth of magnesium-doped indium nitride thin films," *Vacuum*, vol. 155, pp. 16–22, 2018.

[22] H. S. Lee, S. S. Ng, and F. K. Yam, "Effect of nitrogen gas on the growth of magnesium doped indium nitride thin films via sol gel spin coating method," *J. Phys.: Conf. Series.*, vol. 1083, p. 012061, 2018.

[23] H. S. Lee, S. S. Ng, and F. K. Yam, "Doped indium nitride thin films by sol-gel spin coating method," in *AIP Conf. Proc.*, 2017, vol. 1901, p. 020015.

[24] W. K. Wang, S. Y. Huang, M. C. Jiang, and D. S. Wuu, "Optoelectronic properties and structural characterization of GaN thick films on different substrates through pulsed laser deposition," *Appl. Sci.*, vol. 7, no. 1 p. 87, 2017.

[25] A. Taabouche, A. Bouabellou, F. Kermiche, F. Hanini, S. Menakh, Y. Bouachiba, T. Kerdja, C. Benazzouz, M. Bouafia, and S. Amara, "Effect of substrates on the properties of ZnO thin films grown by pulsed laser deposition," *Adv. Mat. Phys. Chem.*, vol. 3, no. 4, pp. 209–213, 2013.

[26] W. C. Chen, S. Y. Kuo, W. L. Wang, J. S. Tian, W. T. Lin, F. I. Lai, and L. Chang, "Study of InN epitaxial films and nanorods grown on GaN template by RF-MOMBE," *Nanoscale Res. Lett.*, vol. 7, no. 1, p. 468, 2010.

[27] R. Graupner, Q. Ye, T. Warwick, and E. Bourret-Courchesne, "Study of interface reactions between Si and GaN at high temperatures using scanning photoelectron microscopy and X-ray absorption spectroscopy," *J. Cryst. Growth*, vol. 217, no. 1–2, pp. 55–64, 2000.

[28] P. P. Chen, H. Makino, T. X. Li, J. B. Wang, W. Lu, and T. Yao, "Optical properties of InN films grown by molecular beam epitaxy at different conditions," *Thin Solid Films*, vol. 513, no. 1–2, pp. 166-169, 2006.

[29] W. Chebil, "Comparison of ZnO thin films on different substrates obtained by sol-gel process and deposited by spin-coating technique," *Indian J. Pure Appl. Phys.*, vol. 53, no. 8, pp .521–529, 2015.

[30] U. Bashi, Z. Hassan, N. M. Ahmed, A. Oglat, and A. S. Yusof, "Sputtered growth of high mobility InN thin films on different substrates using Cu-ZnO buffer layer," *Mater. Sci. Semicond. Process.*, vol. 71, no. 15, pp. 166–173, 2017.

[31] I. Yonenaga, Y. Ohkubo, M. Deura, K. Kutsukake, Y. Tokumoto, Y. Ohno, A. Yoshikawan, and X. Q. Wang, "Elastic properties of indium nitrides grown on sapphire substrates determined by nano-indentation: In comparison with other nitrides," *AIP Adv.*, vol. 5, no. 7, p. 077131, 2015.

[32] B. Liu, T. Kitajima, D. Chen, and S. R. Leone, "Growth modes of InN (000-1) on GaN buffer layers on sapphire," *J. Vac. Sci. Technol., A*, vol. 23, no. 2, pp. 304–309, 2005.

[33] C. Liu, S. H. Chang, T. W. Noh, M. Abouzaid, P. Ruterana, H. H. Lee, D. W. Kim, and J. S. Chung, "Initial growth behavior and resulting microstructural properties of heteroepitaxial ZnO thin films on sapphire (0001) substrates," *Appl. Phys. Lett.*, vol. 90, no. 1, p. 011906, 2007.

[34] A. P. Vajpeyi, S. J. Chua, S. Tripathy, E. A. Fitzgerald, W. Liu, P. Chen, and L. S. Wang, "High optical quality nanoporous GaN prepared by photoelectrochemical etching," *Electrochem. Solid-State Lett.*, vol. 8, no. 4, pp. 85–88, 2005.

[35] V. Y. Davydov, A. A. Klochikhin, M. B. Smirnov, Y. E. Kitaev, A. N. Smirnov, E. Y. Lundina, H. Lu, W. J., Schaff, H. M. Lee, H. W. Lin, Y. L. Hong, and S. Gwo, "SIMS and Raman studies of Mg-doped InN," *Phys. Status Solidi C*, vol. 5, no. 5, pp. 1648–1651, 2008.

[36] E. Ş. Tüzemen, H. Şahin, K. Kara, S. Elagöz, and R. Esen, "XRD, XPS, and optical characterizations of Al-doped ZnO film grown on GaAs substrate," *Turk. J. Phys.*, vol. 38, pp. 111–117, 2014.

[37] C. A. Pan and T. P. Ma, "High-quality transparent conductive indium oxide films prepared by thermal evaporation," *Appl. Phys. Lett.*, vol. 37, no. 2, pp. 163–165, 1980.

[38] M. G. Varnamkhasti, H. R. Fallah, and M. Zadsar, "Effect of heat treatment on characteristics of nanocrystalline ZnO films by electron beam evaporation," *Vacuum*, vol. 86, no.7, pp. 871–875, 2012.

[39] A. O. Mousa, N. F. Habubi, and N. A. Nema, "Substrate effects on structural and optical properties of ZnO thin films deposited by chemical spray pyrolysis," *Int. Lett. Chem. Phys. Astron.,* vol. 51, pp. 69–77, 2015.

[40] H. Kwon, Y. Lee, O. Miki, H. Yamano, and A. Yoshida, "Raman spectra of indium nitride thin films grown by microwave-excited metalorganic vapor phase epitaxy on (0001) sapphire substrates," *Appl. Phys. Lett.*, vol. 69, no.7, pp. 937–939, 1996.

Sha Shiong Ng received his B.Sc. (Hons) degree in Pure Physics, M.Sc. and Ph.D. degrees in Solid State Physics (majoring in semiconductor studies) from Universiti Sains Malaysia (USM), Malaysia.

He served as a senior lecturer in the School of Physics at USM from November 2007 till April 2015. Now, he is attached to Institute of Nano Optoelectronics Research and Technology (INOR), USM. His fields of specialization is growth and characterizations of wide band gap semiconductor materials. He is actively engaged in the researches of (1) III-nitrides based LEDs and solar cells, (2) growth of III-nitrides, metal oxides, and chalcogenide materials, (3) fabrication and characterization of porous/nanostructure thin films, and (4) surface phonon polariton of III-nitrides. Dr. Ng has published more than 150 research papers in Scopus/ISI-indexed journals (h-index = 17; Scopus). Besides, he has filed one patent and published two monographs. At present, Dr. Ng was the principal investigator for 2 international, 5 national, and 5 university research grants. In addition, he was the co-researcher for 16 research grants.

Dr. Ng has received various awards for excellent research. These include the Best Thesis Award, the Best Postgraduate Student Award, the Sanggar Sanjung (Hall of Fame) Awards for publication category. In year 2012, one of his research grants funded under Fundamental Research Grant Scheme has been selected and awarded as the Best Research Project (under Pure Science category) by the Ministry of Higher Education Malaysia. Presently, Dr. Ng is a senior member of Optical Society of America. He is also a member of Materials Research Society, Optical Society of America, The Society for Applied Spectroscopy, and SPIE. Dr. Ng is also a life member of The Malaysian Solid State Science & Technology Society and Malaysian Institute of Physics. Since 2008, he was served as reviewer for many reputable journals.

Hui San Lee was born in Sarawak, Malaysia in 1992. She received the B.S. at University Malaysia Terengganu in Electronic physics and instrumentation. She also continue her M.S. degrees in Research work with title P-type indium nitride thin film grown by sol-gel spin coating technique via nitridation process from the Universiti Sains Malaysia (USM), in 2016.

From 2016 to 2017, she was a Research Assistant with the School of Physics in USM and Nano Optoelectronics Research and Technology (INOR). Since 2007, she has been published few papers with tiltle Influences of Thermal Stability of Doped Indium Nitride Thin Films at Elevated Temperatures by Sol-Gel Spin Coating Method in 3rd Meeting of Malaysia Nitrides Research Group (MNRG 2016) , Doped Indium Nitride Thin Film by Sol-gel Spin Coating Method AIP Conference Proceedings, 3rd Advanced Materials Conference 2016 (AMC2016), Effect of Nitrogen Gas on the Growth of Magnesium Doped Indium Nitride Thin Films via Sol-gel Spin Coating Method in 6th International Conference on Solid State Science and Technolog, and Sol–gel spin coating growth of magnesium-doped indium nitride thin films in Vacuum.

Zhi Yin Lee received her B.Sc (Hons) degree in Applied Physics, M.Sc (Thermal Processes in Device and Packaging) and Ph.D degrees in Solid State Physics (Semiconductor Fabrication – Thin Film) from Universiti Sains Malaysia (USM), Malaysia in 2010, 2013 and 2018, respectively.

At present, she is working as Failure Analysis Engineer at Lumileds Malaysia. Her responsibilities are to identify root cause of electrical, optical and thermal failures in light-emitting diodes, study new techniques to solve technical issue as well as collaborate with functional team for product and process development.